



# A theoretical study on the efficient reversible redox-based switching of the second-order polarizabilities of two-dimensional nonlinear optical-active donor–acceptor phenanthroline-hexamolybdate

Ping Song, Li-Kai Yan, Wei Guan, Chun-Guang Liu, Chan Yao, Zhong-Min Su \*

*Institute of Functional Material Chemistry, Key Laboratory of Polyoxometalate Science of Ministry of Education, Faculty of Chemistry, Northeast Normal University, Changchun 130024, People's Republic of China*

## ARTICLE INFO

### Article history:

Received 9 February 2010

Received in revised form 1 April 2010

Accepted 7 April 2010

Available online 24 April 2010

### Keywords:

Redox-based switching

Second-order NLO response

2D character

Phenanthroline-POMs

Off-diagonal tensor

## ABSTRACT

The  $\Delta$ -shaped phenanthroline-hexamolybdate compounds that are based on the reversible Mo-centered redox process were investigated. The attachment of hexamolybdate terminals to phenanthroline by a  $\pi$ -conjugated phenylamine bridge generated the organic ligand-centered or Ni-centered HOMO and the transition metal Mo-centered LUMO. The population in HOMO and LUMO predicted the reversible  $\text{Mo}^{\text{VI/V}}$  redox process and the ligand-to-metal charge transfer (LMCT) to a polyanion acceptor, which consequently evoked a significant second-order nonlinear optical (NLO) response. Moreover, the electron transition of these compounds exhibited a large  $\beta_{zyy}$  tensor along the y-axis, which confirms a promising two-dimensional (2D) character with sizable anisotropy values. Interestingly, the addition of electrons into the high-valence Mo atom in the hexamolybdate acceptor evoked dramatic enhancements in the NLO response for the reduction states in contrast to the response of the corresponding oxidation states. The reduction states in system **I** exhibited second-order NLO responses about 200 times larger than the oxidation states. In addition, the attachment of the Ni atom in compound **IIa<sub>red</sub>** enhanced the NLO response to nearly 1019 times greater than the response of the corresponding oxidation state compound **IIa**. The Ni atom as the electron donor plays an important role in the major electron transition for the reduction states in system **II**. Therefore, the NLO response of such compounds can be reversibly switched through the transition metal  $\text{Mo}^{\text{VI/V}}$  redox that is effectively coupled with the LMCT transition. Thus, the NLO activity can be controlled by a one-electron redox process, and the redox-active phenanthroline-hexamolybdate compounds are promising candidates for 2D redox-switching NLO materials in novel optoelectronic applications.

© 2010 Elsevier Inc. All rights reserved.

## 1. Introduction

Polyoxometalates (POMs) are anionic clusters of discrete structure that are commonly based on molybdenum or tungsten oxides. In most cases, the practical applications of POMs in many areas depend on their redox properties, photochemical responses and various other characteristics [1]. Because POMs are highly thermally stable, they offer a wide range of transition metals with different coordination states. The properties of POMs can be enhanced or modified by introducing secondary functional groups (e.g., the covalent attachment of organic/organometallic moieties to the metal-oxo framework), which allows the interplay between d electrons of the cluster and the organic delocalized  $\pi$ -electron to be explored at the molecular level. Delocalized electrons coexist in both the organic network and the inorganic clusters. Over the

past few years, more attention has been paid to the organic-POM hybrid materials [2] that are covalently formed by the insertion of organometallic compounds into the lacunary POMs or by the linkage of the organic and inorganic components using covalently linked POMs and organic polymers [3]. Among the hybrid materials, specific POM-terminal molecules, which contain two POM segments that are covalently connected by an extended  $\pi$ -conjugated bridge, display interesting medicine and biological potentials with respect to their unique electrochemical, magnetic, catalytic, antimicrobial and antitumor properties [4].

The potential synergistic effects of organic-POM hybrid materials may generate strong electronic communications, which could potentially allow the covalent grafting of electron-accepting POMs into an organic conjugated polymer to construct promising nonlinear optical (NLO) materials. In addition, various blocks can be built by combing the parent and the  $\pi$ -conjugated or non-conjugated organic groups. The NLO responses for the organic derivatives of hexamolybdates were previously investigated, and it was confirmed that intramolecular electron transfers occur in

\* Corresponding author. Fax: +86 431 85684009.

E-mail address: [zmsu@nenu.edu.cn](mailto:zmsu@nenu.edu.cn) (Z.-M. Su).

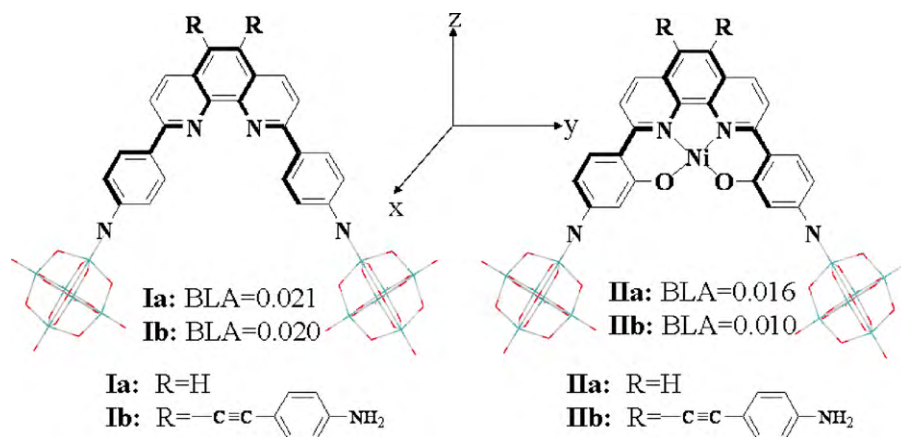


Fig. 1. The calculated  $\Lambda$ -shaped phenanthroline-POM models with 2D characters.

such donor–acceptor (D–A) materials, which results in large NLO responses [5]. The molecular optical nonlinearities of such simple dipolar species are primarily one-dimensional (1D) NLO materials (i.e. dominated by one  $\beta$  tensor component). In recent years, multi-dimensional second-order NLO materials have attracted more attention because they offer the advantage of a better nonlinearity/transparency tradeoff. The substitution of the terminal oxygen in the POM cluster by organoimido ligands provides effective approaches to develop two-dimensional (2D)  $\Lambda$ -shaped structures with  $C_{2v}$  symmetry. These  $\Lambda$ -shaped molecules exhibit significant second-order NLO responses with larger off-diagonal  $\beta$  tensors comparing with 1D NLO materials.

Recently, NLO switching materials have received a lot of attention because the incorporation of switchability into NLO behavior may lead to exciting and novel developments in photonic materials [6]. The ability to reversibly switch the NLO response of a molecule from “on” to “off” by a simple controllable modification would significantly enhance the utility of NLO molecules and consequently influence the development of molecular photonic devices whose properties could be switched by modifying one of the component parts. Photoswitching has recently gained popularity as an effective method used to exhibit a change in NLO responses [7]. Another more attractive method of adjusting the second-order NLO responses of molecules is the use of facile reversible metal-centered redox processes, which reduce the acceptor capacity of the acceptor moiety or enhance the donor effect of the donor moiety. Complexes that contain redox-active metal centers could potentially serve as excellent switchable NLO materials.

The NLO switching response has been achieved by the reversible electron-deficient  $\text{Ru}^{\text{III/II}}$  redox couple [8]. An important and common application of POMs with favorable oxidation potentials and reactive transition metal centers is based on their potentials as electron acceptors and their usefulness in electron transfer oxidation reactions and in the activation of oxygen donors [9]. Interestingly, most POMs exhibit reversible electrochemical behaviors, and their redox properties, which allow them to undergo one or several electron reductions, have provided an attractive platform for the development of catalysts without significantly deforming the POM framework [10]. The reversible redox coupling at modest potentials provides an ideal route for redox-based switching of second-order NLO responses. Therefore, switchable NLO materials can be identified by combining attractive redox properties and NLO responses of POM-based hybrid derivatives that display a remarkable NLO response [11], which constitutes a more effective approach for modulating NLO responses and designing redox-switchable NLO materials.

In the current study, the  $\Lambda$ -shaped hybrid phenanthroline-polyoxometalate compounds originating from the introduction of redox-active hexamolybdate into  $\pi$ -donor-substituted phenanthroline were investigated, and the calculated models are shown in Fig. 1. The molecular geometries for all the studied compounds were optimized under  $C_{2v}$  symmetry. Quantum chemistry programs use the so-called “standard orientation” for a  $C_{2v}$  group, which assigns the z axis to the  $C_2$  axis of symmetry, and the molecule is then placed on the zy plane with the x axis orthogonal to the molecule (as shown in Fig. 1). As a whole, the compounds with  $C_{2v}$  symmetry have a permanent dipole moment in the direction of the principal axis of the symmetry.

## 2. Computational details

The density functional theory (DFT) method was performed with the ADF2008.01 programs [12–14]. Zero-order regular approximations (ZORAs) were adopted in all the calculations to account for the scalar relativistic effects [15,16], and the local density approximation (LDA), which was characterized by Vosko–Willk–Nusair (VWN) [17] parametrization, was adopted for the correlation functional. Furthermore, the supplemental generalized-gradient approximation (GGA) was employed in the geometry optimizations by using the Becke [18] and Perdew [19] exchange–correlation (XC) functional. Triple- $\xi$  plus polarization Slater basis sets, which were applied with the frozen core approximation, were taken to describe the electrons of the main group elements (O, C, N and H) and the valence electrons of the transitional metal atoms (Mo and Ni). For the main group elements (O, N and C), the frozen core approximation was used up to the 1s shell, while for the transition metal Mo atom and the Ni atom, the frozen core approximation was used up to the 3d and 2p shells, respectively. A solvent model, the conductor-like screening model (COSMO) [20], was employed with the dielectric constants of  $\epsilon = 37$  (N,N-dimethylformamide, DMF). The Van der Waals radii for the POM atoms, which actually define the cavity in the COSMO, were 1.4, 1.41, 1.49, 1.08, 2.09 and 1.84 Å for O, N, C, H, Mo and Ni, respectively [21]. As it is one of the most popular methods for the calculation of excitation properties, time-dependent density functional theory (TD-DFT) was employed as an effective method to calculate the excitation properties, which included closed- and open-shell systems. Compared to traditional local density approximation (LDA) and GGA potentials, three different functionals for the zeroth-order potential (“van Leeuwen–Baerends (LB94) XC potential” by van Leeuwen and Baerends [22], “statistical average of orbital potentials” (SAOP) by Gritsenko, Baerends and co-workers

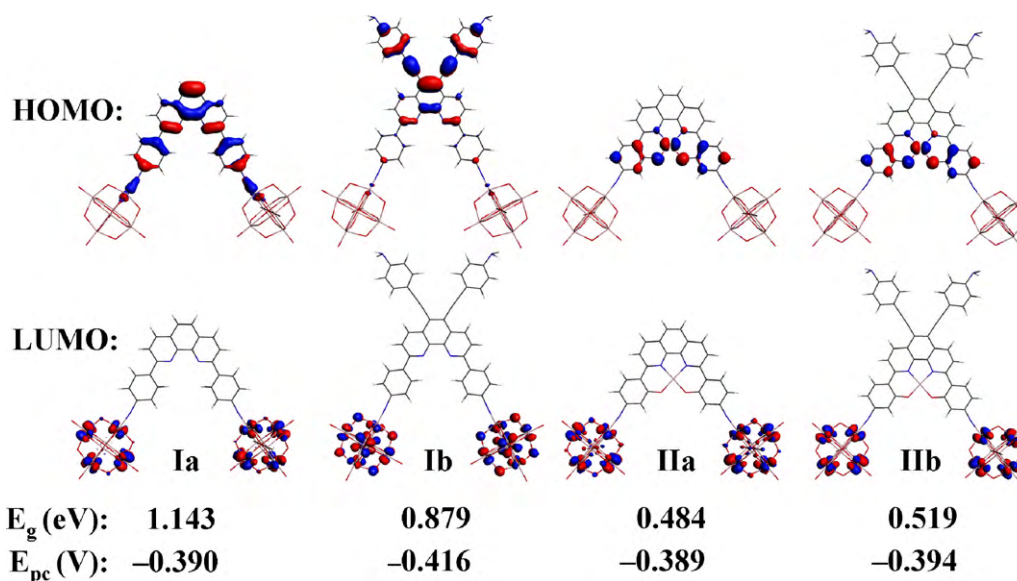


Fig. 2. The frontier molecular orbitals for the compounds used in this study with the corresponding energy gaps and reduction potentials.

[23] and the “gradient-regulated connection potential” (GRAC) [24]) show superior results in spectrum properties. In particular, the SAOP and the GRAC correct the Kohn–Sham potential in the outer “asymptotic” region and thus lead to improved virtual orbitals and virtual orbital energies. The GRAC constructs also smooth asymptotically corrected potentials that are genuine density functionals with an analytical representation. Moreover, previous studies indicated that the GRAC may be the most suitable functional for large POM systems [25]. Based on these previous findings, we adopted the TDDFT in addition to the GRAC potential to calculate the electron transitions in the current study. The finite field (FF) approach was executed to calculate the second-order polarizability [26]. All the calculations were performed from solutions containing N,N-dimethylformamide (DMF).

### 3. Results and discussion

#### 3.1. Redox properties

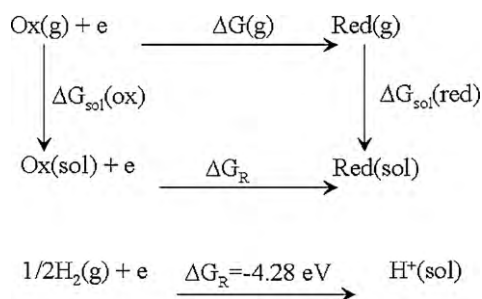
The compounds used in this study resemble shoulder poles carrying hexamolybdate baskets that are covalently attached to the 2 and 9 positions of the phenanthroline ligand by a  $\pi$ -conjugated phenylamine bridge linkage. Based on the results presented in Fig. 2, the HOMO for compound **Ia** is a  $\pi$ -orbital character that perfectly delocalizes over the whole organic segment, while the LUMO has a larger amount of nonbonding d-Mo orbitals in the polyanion where the oxo band and the empty set of d-metal orbitals are perfectly separated. When the two hydrogen atoms at the **R** position on the periphery of the phenanthroline ring in compound **Ia** were replaced by a strong electron-donating 4-ethynylbenzenamine group, the  $\pi$  electrons contributed to the HOMO in compound **Ib** were assigned to the phenyl rings that were adjacent to amido donor. The LUMO of compound **Ib** is characterized by the major d-Mo orbitals while the bridge oxygen atoms distinguish part of the p-orbital. The Ni-phenanthroline-POM compounds **IIa** and **IIb**, which contain the transition metal Ni atom attached into the organic moiety, are shown in Fig. 1. The transition metal Ni-centered HOMO with the  $\pi$ -type orbital over the adjacent phenol ring and the pure Mo-centered LUMO in compound **IIa** potentially generate large electron transitions. The HOMO in compound **IIb** is the same as that in compound **IIa**, which is different from the HOMO

over the electron-donating group in compound **Ib**. The transition metal Ni atom in system **II** plays an essential role in modifying the HOMO and promoting the HOMO energy to induce a lower energy gap than the gap observed in system **I**. The redox properties of the compounds heavily depend on the energy and the composition of the LUMO orbitals. Consequently, the one-electron reduction that occurs on the nonbonding d-Mo orbital in the POM moiety may generate slightly more active redox properties in system **II** than in system **I**. Among these properties, the first reduction potential for compound **Ib** may be slightly different from the other three compounds due to the partial participation of bridge oxygen atoms in the LUMO population. In addition, the frontier molecular orbital (FMO) infers that the preferred electron transitions of the POM-based compounds will be from organic segments to polyanions.

According to the FMO analysis in Fig. 2, phenanthroline-POM compounds are composed of two electroactive hexamolybdate acceptor units that are linked by a bis-2,9-di(4-aminophenyl)-1,10-phenanthroline donor bridge. Within the compounds, the hexamolybdate moiety potentially displays a significant effect on the electronic properties, and the redox property is closely related to hexamolybdate. Basically, phenanthroline-POM compounds involve one electron that is added to a mostly nonbonding metal Mo orbital and are preferentially reduced in the Mo centers, which is in accord with the electrochemical studies [4b]. In order to facilitate chemical redox studies, the electrochemical behavior of the compounds in this study was reproduced, and the first redox behavior was considered in DMF. The theoretical prediction of the redox potential of a given compound requires the determination of the free energy that is associated with the following thermodynamic cycle, which is outlined in Scheme 1.

Since the calculation of the vibrational frequencies is still unfeasible for large molecules like POMs, the frequency calculations were ignored as in previous reports [27–29], and the  $\Delta G_R$  in the equation  $E^\circ = -\Delta G_R/nF$  was approximated as the reduction energy of the POMs in solution ( $n = 1$  for the one-electron reduction). The  $E^\circ$  values were measured and compared to a reference electrode, NHE (normal hydrogen electrode), and the free energy change for the half-reaction  $1/2H_2 \rightarrow H^+ + e^-$  was estimated to be  $-4.28$  eV [30].

As shown in Fig. 2, the first one-electron reductions in compounds **Ia** and **IIa** occur at approximately equal values of  $-0.39$  V, which correlates with the experimental value for compound **Ia** ( $-0.51$  V) [4b]. When the electron-donating 4-



**Scheme 1.** The thermodynamic cycle for simulating the Gibbs free energy.

ethynylbenzenamine group replaced the two hydrogen atoms at the **R** position of the phenanthroline, a slight anodic-shift of 0.026 V and 0.005 V was observed for the first reduction potentials in compounds **1b** and **11b**, respectively, which corresponds to the FMO predictions for similar redox properties.

### 3.2. Second-order polarizabilities

Bond length alternation (BLA) can be used as a complementary tool to represent the extent of electron delocalizations along the conjugated bridge, and the term  $\Delta r$  is defined as the average change in length between adjacent single and double bonds [31]. As an important organic NLO chromophore, the ground-state structure for the donor–acceptor substituted polyene molecule is viewed as a combination of two resonance forms that differ in their levels of charge separation [32,33]. When the donor and acceptor substituents that are connected by the conjugated bridge become stronger, the contributions of the charge-separated resonance forms to the ground state of the molecule increase and the BLA values decrease. Thus, BLA values are significant factors that help define NLO responses. In Fig. 1, the  $\Delta r$  for compound **1a** is 0.021 when the hexamolybdate has attached to the 2 and 9 positions of the phenanthroline by a  $\pi$ -conjugated phenylamine bridge linkage. For compound **11a**, the  $\Delta r$  is lower, 0.016, which is likely due to the incorporation of the Ni transition metal into the phenanthroline. Modifications of the electron-donating groups in compounds **1b** and **11b** evoke lower BLA values of 0.020 and 0.018, respectively, which contrast with the corresponding values of compounds **1a** and **11a**. Based on these results, the incorporation of the polyoxometalate with strong electron-donating groups enhances the electron delocalization and increases the contribution of charge-separated resonances, which results in an enhancement of the NLO properties.

The total second-order polarizabilities  $\beta_0$  for the studied compounds are defined in the following equation:

$$\beta_0 = (\beta_x^2 + \beta_y^2 + \beta_z^2)^{1/2} \quad (1)$$

$\beta_x$ ,  $\beta_y$  and  $\beta_z$  are the components of the second-order polarizability tensor along the  $x$ -,  $y$ - and  $z$ -axes, respectively. The vector component of  $\beta$  ( $\beta_i$ ) is defined by the equation shown below (2):

$$\beta_i = \beta_{iii} + \frac{1}{3} \sum_{j \neq i} (\beta_{ijj} + \beta_{jij} + \beta_{jji}) \quad (2)$$

Herein,  $\beta_{iii}$  is the diagonal tensor. For a chromophore with  $C_{2v}$  symmetry, there are five nonzero components of the  $\beta$  tensor,  $\beta_{zzz}$ ,  $\beta_{zyy}$ ,  $\beta_{zxx}$ ,  $\beta_{yyz}$  and  $\beta_{xxz}$ . Assuming Kleinman symmetry,  $\beta_{zyy} = \beta_{yyz}$  and  $\beta_{zxx} = \beta_{xxz}$ . Therefore, if we assume a single substantial 2D structure, then  $\beta_{zxx} = \beta_{xxz} = 0$ , and only the diagonal tensor  $\beta_{zzz}$  and the off-diagonal tensor  $\beta_{zyy}$  are the crucial tensor components. The total  $\beta_0$  and the corresponding  $\beta_{zzz}$  and  $\beta_{zyy}$  tensor components are shown in Table 1. The results indicate that the phenanthroline-

POMs exhibit significant NLO responses. The phenanthroline-POM compound **1a**, which may exhibit a large ligand-to-metal charge transfer (LMCT) that was based on an FMO analysis and due to the attachment of the POM moiety, displays a significant  $\beta_0$  of up to  $614.9 \times 10^{-30}$  esu. In addition, the incorporation of the Ni atom into compound **11a** reduces the  $\beta_0$  value by about 50% in comparison to the value for compound **1a**. In contrast, substitution of the H atoms at the **R** position in compounds **1b** and **11b** with the powerful electron-donating 4-ethynylbenzenamine group significantly increases the  $\beta_0$  values to more than twice the values of the corresponding compounds **1a** and **11a**. The typical NLO *p*-nitroaniline (PNA) material with the  $D-\pi-A$  model was chosen as a reference molecule, and the calculated NLO response using the finite field (FF) method was  $15.5 \times 10^{-30}$  esu, which correlates with the experimental value of  $12.1 \times 10^{-30}$  esu [34]. Though there were no experimental values, the relatively large NLO responses of the phenanthroline-POM compounds compared to PNA indicate their promising applications in NLO materials.

In order to examine the 2D character of the nonlinearity for the compounds in this study, the “in-plane nonlinear anisotropy” value ( $u$ ), which is defined as the ratio  $u = \beta_{zyy}/\beta_{zzz}$  [35], was introduced. The  $u$  value is a very sensitive function of the off-diagonal tensor components and a relevant parameter for describing the 2D character of the compounds’ molecular NLO responses. The  $\Lambda$ -shaped molecules were previously reported to exhibit transparent and phase-matchable noncentrosymmetric structures in which the large off-diagonal  $\beta$ -tensor components were responsible for the large second-order NLO responses. In addition, off-diagonal  $\beta$  tensors were related to the charge-transfer transitions that were polarized perpendicular to the molecular dipolar axis, while the diagonal  $\beta$  tensor mainly contributed to the parallel transitions.

The  $u$  value for compound **1a**, which contains two hexamolybdate terminals, is 0.65, indicating the 2D character of the charge transfer is favored. The incorporation of the Ni atom into compound **11a** weakened the parent 2D character, as indicated by a decreased anisotropy value  $u$  of 0.44, which is still high enough to retain a 2D character. In contrast, the anisotropy values were reduced to 0.51 and 0.32 in compounds **1b** and **11b**, respectively, due to a departure from the planarity of the pyramid amido with the electron-donating 4-ethynylbenzenamine substitution. Compounds **1b** and **11b** likely do not exhibit relatively significant 2D NLO properties when compared to the corresponding unsubstituted compounds **1a** and **11a**, while they still display typical values of 2D donor–acceptor bis(salicylaldiminato)Ni<sup>II</sup> Schiff base complexes (NiL) and the related ligands ( $H_2L$ ) [36].

To further reveal the origin of the second-order NLO properties of the compounds used in this study, the elucidation of the structure–property relationship is necessary. For large second-order NLO responses of phenanthroline-POM compounds, the crucial electron transition features have been investigated. Only the “in-plane”  $y$ -polarized and  $z$ -polarized transitions are allowed for the molecules with  $C_{2v}$  symmetry. The  $y$ -polarized transition contributes to the off-diagonal second-order polarizability tensor, while the  $z$ -polarized transition accounts for the diagonal tensor (the  $z$ -axis being the principal one).

Based on FMO analyses, the hexamolybdate moiety is a powerful electron-withdrawing group that engages in visible LMCT excitations when it is attached to the phenanthroline by a  $\pi$ -conjugated phenylamine bridge linkage. As shown in Fig. 3, the molecular orbital (MO) analysis in compound **1a** exhibits two main transitions from the  $\pi$ -type 44b1 orbital (orthogonal to the plane defined by the whole organic conjugated segment with part of the  $\pi$ -orbital for the Mo–N bond) into the POM-based 49a2 and 50a2 states, which are mainly composed of the d-Mo orbital in the polyanion and a small part of the Mo–N  $\pi$ -orbital, respectively. Importantly, the two main LMCT transitions for compound **1a** are based on the



**Table 1**

The calculated total second-order polarizabilities ( $\beta_0 \times 10^{-30}$  esu), tensors ( $\beta_{zyy}, \beta_{zyy} \times 10^{-30}$  esu), anisotropies ( $u$ ) and main electron transitions of the compounds used in this study.

Model	$\beta_{zyy}$	$\beta_{zzz}$	$u$	$\beta_0$	Symmetry <sup>a</sup>	$E$	$f$	Main transition
<b>Ia</b>	241.4	371.2	0.65	614.9	B2(y)	1.863	0.145	44b1 $\rightarrow$ 49a2 (94%)
					B2(y)	2.322	0.287	44b1 $\rightarrow$ 50a2 (80%)
<b>Ib</b>	460.8	906.4	0.51	1370.6	B2(y)	1.990	0.166	49b1 $\rightarrow$ 55a2 (80%)
					A1(z)	2.116	0.284	49b1 $\rightarrow$ 56b1 (40%), 48a2 $\rightarrow$ 54a2 (34%)
<b>IIa</b>	102.7	231.7	0.44	335.9	B2(y)	1.931	0.157	46b1 $\rightarrow$ 51a2 (90%)
<b>IIb</b>	343.8	451.8	0.76	798.3	A1(z)	1.660	0.062	52b1 $\rightarrow$ 58b1 (95%)

<sup>a</sup> The symbols in the parentheses represent the polarization direction.

off-diagonal polarizability tensor that is polarized perpendicular to the molecular dipolar axis. The participation of the Ni metal atom in the Ni-phenanthroline-POM compound **IIa** plays no significant role in the crucial electron transition, which is mainly formed by the contribution of 46b1  $\rightarrow$  51a2 with respect to the perpendicular  $y$ -polarized transition from the  $\pi$ -type organometallic complex segment to the polyanion framework.

The lowest-lying energy transition with an electron-donating effect in compound **Ib** is polarized along the  $y$ -axis at the B2 symmetry with the charge transfer of 49b1  $\rightarrow$  55a2, which originates from the delocalized  $\pi$  electrons over the **R** group to the d-Mo orbital. The second lowest-lying energy transition in compound **Ib** has the A1 symmetry with the major electron transitions assigned to 49b1  $\rightarrow$  56b1 and 48a2  $\rightarrow$  54a2, which mainly arise from delocalized  $\pi$  electrons over the **R** group (49b1) and the bis-2,9-di(4-aminophenyl)-1,10-phenanthroline with the  $\pi$ -orbital of the Mo–N bond (48a2) to the d-Mo orbital. For this energy transition, the  $\pi$ -orbital for the Mo–N bond lies along the  $z$ -axis. In contrast to the main transition that polarizes along the  $y$ -axis in compound **Ia**, the charge transfer component in compound **Ib** is polarized along the  $z$ -axis and consequently reduces the  $\beta_{zyy}$  tensor component in the ratio  $u = \beta_{zyy}/\beta_{zzz}$ , which generates a smaller  $u$  value. The electron-donating effect strengthens the charge separation, and the large degree of charge transfer results in a greater  $\beta_0$  value than the value of compound **Ia**. The major electron transition in compound **IIb** is similar to the lowest energy transition in compound **Ib** where the charge transfer is assigned to 52b1  $\rightarrow$  58b1 with A1 symmetry along the  $z$ -axis contributed by the delocalized  $\pi$  electrons over the **R** group to the d-Mo orbital.

The phenanthroline-POM derivatives exhibit significant LMCT transitions, and they are ideally suited towards redox-switching of the NLO responses due to their completely reversible one-electron couplings at readily accessible potentials. The reduction effects on second-order NLO properties were investigated in this study. The values listed in Table 2 suggest that the  $\beta_0$  values are strongly dependent on the incorporation of an extra electron. The  $\beta_0$  value for the one-electron reduced compound **Ia<sub>red</sub>** dramatically increases to  $115124.3 \times 10^{-30}$  esu, which is approximately 187-fold higher than corresponding value of oxidation state compound **Ia**. Similarly, the  $\beta_0$  value for compound **IIa<sub>red</sub>** increases nearly 1019-fold to  $342212.1 \times 10^{-30}$  esu when compared to the value of compound **IIa**. Though the oxidation state **IIa** compound shows a lower  $\beta_0$  value than the oxidation state compound **Ia**, the attachment of the Ni atom significantly enhances the NLO response for the corresponding reduction state. This result suggests that the Ni atom considerably contributes to the main electron transition. Interestingly, the  $\beta_0$  value for the reduction state compound **Ib<sub>red</sub>** with the electron-donating effect is enhanced to  $297553.5 \times 10^{-30}$  esu, which is 217 times greater than the value of the corresponding oxidation state compound **Ib** and nearly 2.5 times greater than the value of compound **Ia<sub>red</sub>**. The  $\beta_0$  value of compound **IIb<sub>red</sub>**,  $180930.3 \times 10^{-30}$  esu, is 227 times larger than the value of compound **IIb**. These combined results indicate the NLO response is reversibly switched by the presence of a redox-active metal center. The NLO property is “on” in the reduction state and “off” in the corresponding oxidation state.

A particularly interesting result shown in Table 2 is that the low-lying electron transitions for the reduced POM-based compounds are generally composed of a single principal state. The main

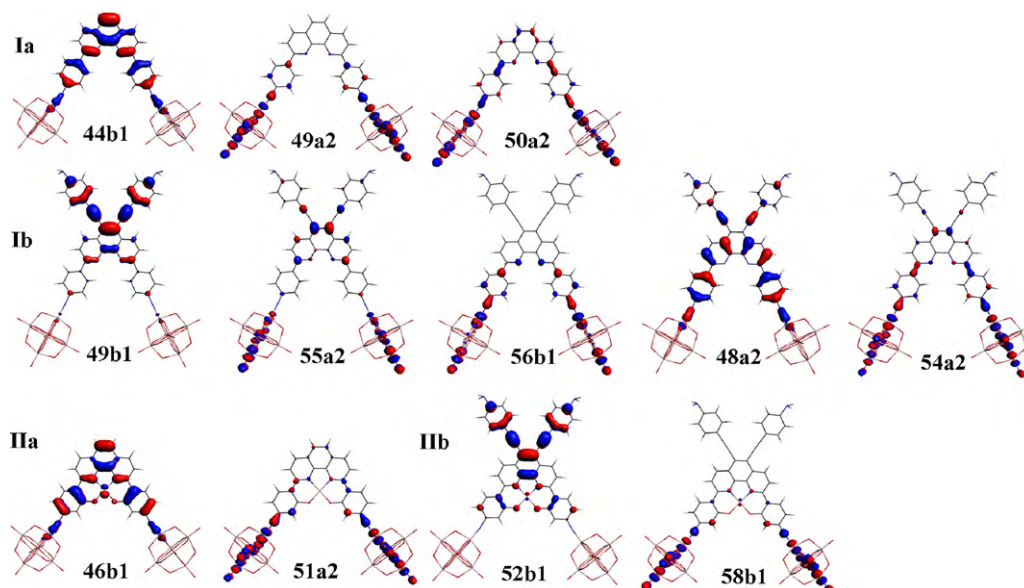


**Fig. 3.** The major electron transitions for the oxidized compounds in systems **I** and **II**.

**Table 2**The calculated total second-order polarizabilities ( $\beta_0 \times 10^{-30}$  esu) and main electron transitions for the reduction compounds.

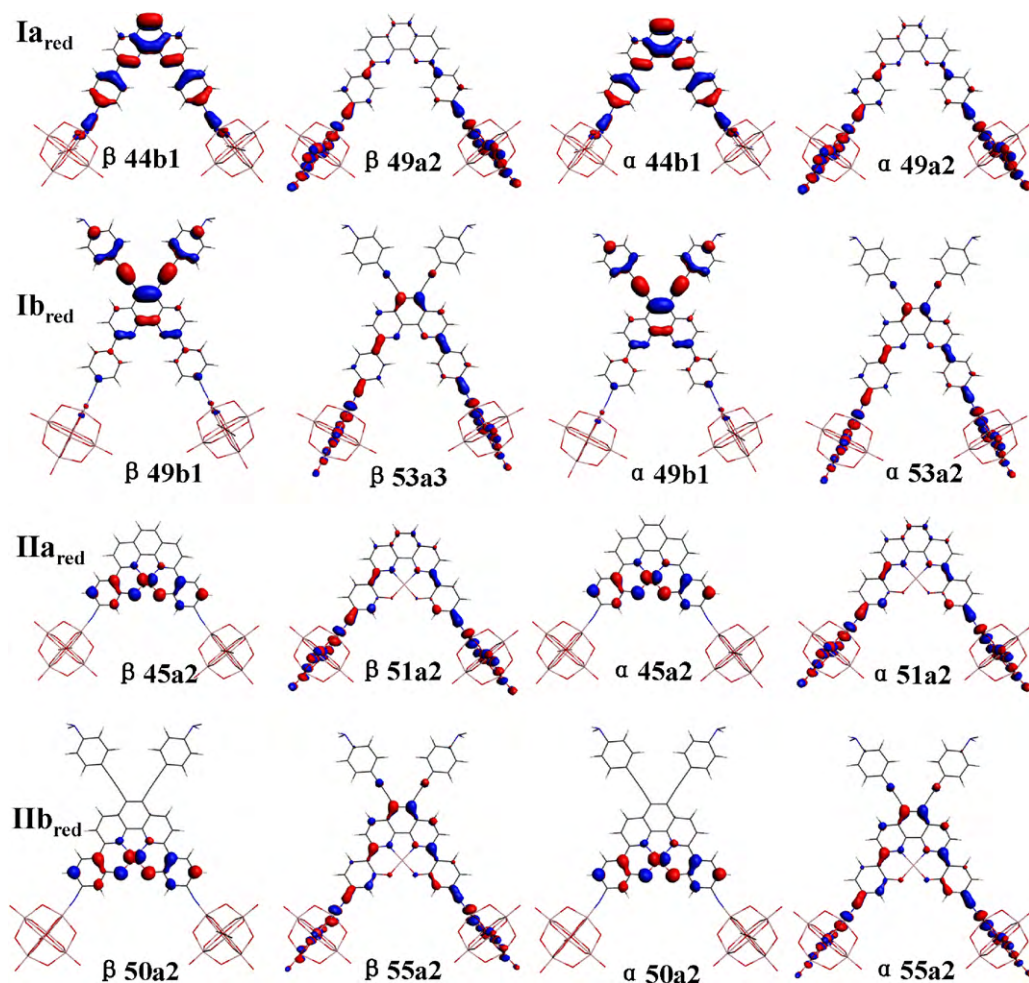
Model	$\beta_0$	Symmetry <sup>a</sup>	$E$	$f$	Main transition
<b>Ia<sub>red</sub></b>	115124.3	B2(y)	1.952	0.169	$\beta 44b1 \rightarrow 49a2$ (48%), $\alpha 44b1 \rightarrow 49a2$ (42%)
<b>Ib<sub>red</sub></b>	297553.5	B2(y)	1.696	0.164	$\beta 49b1 \rightarrow \beta 53a2$ (46%), $\alpha 49b1 \rightarrow \alpha 53a2$ (40%)
<b>IIa<sub>red</sub></b>	342212.1	A1(z)	1.272	0.008	$\beta 45a2 \rightarrow 51a2$ (57%), $\alpha 45a2 \rightarrow 51a2$ (32%)
<b>IIb<sub>red</sub></b>	337336.3	A1(z)	1.251	0.038	$\beta 50a2 \rightarrow 55a2$ (58%), $\alpha 50a2 \rightarrow 55a2$ (38%)

<sup>a</sup> The symbols in the parentheses represent the polarization direction.

electron transitions of the corresponding reduced compounds are shown in Fig. 4. When comparing the two crucial CT transitions along the y-axis from the organic conjugated plane to the polyanion at the terminals in compound **Ia**, the electron added to the POM acceptor in compound **Ia<sub>red</sub>** reduces the acceptor capacity. In compound **Ia<sub>red</sub>**, the only major electron transition along the y-axis that plays a significant role is based on equal components of  $\beta 44b1 \rightarrow 49a2$  and  $\alpha 44b1 \rightarrow 49a2$ , which are both found from the  $\pi$ -conjugated organic segment to the inorganic polyanion. Remarkably, the main electron transition in compound **IIa<sub>red</sub>** is composed of  $\beta 45a2 \rightarrow 51a2$  and  $\alpha 45a2 \rightarrow 51a2$  along the z-axis, which is very different from the transition that occurs primarily along the y-axis in the oxidation compound **IIa**. Moreover, the electron donors for compound **IIa<sub>red</sub>** are the Ni atom and the adjacent phenol ring, which are not involved in compound **IIa**.

The addition of the electron to compound **Ib** evokes nearly equivalent contributions (about 45%), and the components of the

lowest energy electron transition consist of  $\beta 49b1 \rightarrow 53a2$  and  $\alpha 49b1 \rightarrow 53a2$ , which originate from the delocalized  $\pi$  electrons over the **R** group to the d-Mo orbital with part of the Mo–N bond. The composition of this transition is similar to the population with the lowest energy transition in compound **Ib**. In contrast, the electron donor of compound **IIb<sub>red</sub>** is the Ni atom with the phenol ring ( $\beta 50a2$  and  $\alpha 50a2$ ) rather than the **R** group like in compound **IIb**, and the electron transfers to the d-Mo orbital with part of the Mo–N bond ( $\beta 55a2$  and  $\alpha 55a2$ ) along the z-axis. Clearly, the transition metal Ni within organometallic complexes significantly contributes to the frontier molecular orbitals in the Ni-phenanthroline-POM compounds and the electron transitions in the reduction states. These transition characters for the oxidation and reduction states are all assigned to the LMCT where the Ni atom is involved in the ligand, and they may provide information about the influence of the metal-centered redox process in the intramolecular donor and acceptor characters, which results in the variations in the  $\beta$  values.

**Fig. 4.** The major electron transitions for the reduced compounds in systems **I** and **II**.

## 4. Conclusions

The current study characterized the family of 2D dipolar NLO phenanthroline-POMs based on redox-switchable transition metal centers in the POM segment. The incorporation of hexamolybdates that are linked through the Mo–N bond and act as the terminals of the  $\Lambda$ -shaped systems generates larger charge transfers to the polyanion acceptor and consequently creates significantly large second-order NLO responses. The electron transitions in the phenanthroline-POMs exhibit large  $\beta_{zyy}$  tensors along the  $y$ -axis, which confirms the presence of more favorable 2D characters with sizable anisotropy values. The electron-donating effect of the substituent in the phenanthroline-POM compounds causes larger charge separations that are accompanied by larger NLO responses in comparison to unsubstituted compounds. Interestingly, the addition of electrons into the high-valence metal Mo in the POM acceptor dramatically enhances the NLO responses for the reduction states, which is in contrast to the responses for the corresponding oxidation states. Compound **IIa<sub>red</sub>** exhibits a second-order NLO response that is nearly 1019 times greater than that of compound **IIa** because of the addition of the Ni atom. Therefore, the NLO activity of such compounds can be reversibly and effectively switched with the presence of the transition metal Mo<sup>VI/V</sup> redox couple in the hybrid redox-active phenanthroline-POMs, and these compounds are very promising candidates for redox-switching NLO applications. The reversibility of active redox couples at readily accessible potentials provides extensive opportunities for the modulation of NLO responses, and this study represents an example of switching the NLO responses by controlling the corresponding oxidation and reduction states. This approach has obvious potential for the switching of bulk NLO effects in electrode-deposited films, and these materials that exhibit switchable NLO properties possess various novel optoelectronic applications.

## Acknowledgments

The authors gratefully acknowledge the financial support from the National Natural Science Foundation of China (project no. 20971020), the Program for Changjiang Scholars and the Innovative Research Team at the University (IRT0714), the Department of Science and Technology of the Jilin Province (20082103), the Training Fund of NENU's Scientific Innovation Project (STC07017), and the Science Foundation for Young Teachers of Northeast Normal University (20090401). We also acknowledge YHK for computational support.

## References

- [1] D.E.A. Katsoulis, Survey of applications of polyoxometalates, *Chem. Rev.* 98 (1998) 359–387.
- [2] M.T. Pope, *Heteropoly and Isopoly Oxometalates*, Springer, New York, 1983.
- [3] (a) H. Zeng, G.R. Newkome, C.L. Hill, Poly(polyoxometalate) dendrimers: molecular prototypes of new catalytic materials, *Angew. Chem., Int. Ed.* 39 (2000) 1771–1774; (b) C. Sanchez, G.J. de, A.A. Soler-Illia, F. Ribot, Y. Lalot, C.R. Mayer, V. Cabuil, Designed hybrid organic–inorganic nanocomposites from functional nanobuilding blocks, *Chem. Mater.* 13 (2001) 3061–3083; (c) Z. Peng, Rational synthesis of covalently bonded organic–inorganic hybrids, *Angew. Chem., Int. Ed.* 43 (2004) 930–935; (d) A. Proust, R. Thouvenot, P. Gouzerh, Functionalization of polyoxometalates: towards advanced applications in catalysis and materials science, *Chem. Commun.* (2008) 1837–1852; (e) Q. Li, L.S. Wang, P.C. Yin, Y.G. Wei, J. Hao, Y.L. Zhu, L. Zhu, G. Yuan, Convenient syntheses and structural characterizations of mono-substituted alkylimido hexamolybdates: [Mo<sub>6</sub>O<sub>18</sub>(NR)]<sup>2−</sup> (R = Me, Et, n-Pr, i-Pr, n-Bu, t-Bu, Cy, Hex, Ode), *Dalton Trans.* (2009) 1172–1179; (f) S. Reinoso, L. Fernando Piedra-Garza, M.H. Dickman, A. Praetorius, M. Biesemans, R. Willem, U. Kortz, Trilacunary A- $\beta$ -Keggin tungstogermanates and -silicates functionalized with phenyltin(IV) electrophiles, *Dalton Trans.* 39 (2010) 248–255.
- [4] (a) M. Lu, Y.G. Wei, B.B. Xu, C. Fung-Chi Cheung, Z.H. Peng, D.R. Powell, Hybrid molecular dumbbells: bridging polyoxometalate clusters with an organic  $\pi$ -conjugated rod, *Angew. Chem., Int. Ed.* 41 (2002) 1566–1568; (b) I. Bar-Nahum, K.V. Narasimulu, L. Weiner, R. Neumann, Phenanthroline-polyoxometalate hybrid compounds and the observation of intramolecular charge transfer, *Inorg. Chem.* 44 (2005) 4900–4902; (c) Y. Zhu, L.S. Wang, J. Hao, Z.C. Xiao, Y.G. Wei, Y. Wang, Synthetic, structural, spectroscopic, electrochemical studies and self-assembly of nanoscale polyoxometalate-organic hybrid molecular dumbbells, *Cryst. Growth. Des.* 9 (2009) 3509–3518.
- [5] (a) L.K. Yan, M.S. Jin, J. Zhuang, C.G. Liu, Z.M. Su, C.C. Sun, Theoretical study on the considerable second-order nonlinear optical properties of naphthylimido-substituted hexamolybdates, *J. Phys. Chem. A* 112 (2008) 9919–9923; (b) M.R.S.A. Janjua, C.G. Liu, W. Guan, J. Zhuang, S. Muhammad, L.K. Yan, Z.M. Su, Prediction of remarkably large second-order nonlinear optical properties of organoimido-substituted hexamolybdates, *J. Phys. Chem. A* 113 (2009) 3576–3587; (c) C.G. Liu, W. Guan, L.K. Yan, Z.M. Su, P. Song, E.B. Wang, Second-order nonlinear optical properties of transition-metal-trisubstituted polyoxometalate-diphosphate complexes: a donor-conjugated bridge-acceptor paradigm for totally inorganic nonlinear optical materials, *J. Phys. Chem. C* 113 (2009) 19672–19676.
- [6] (a) J.-M. Lehn, *Supramolecular Chemistry: Concepts and Perspectives*, VCH, Weinheim, 1995; (b) M.D. Ward, Metal-metal interactions in binuclear complexes exhibiting mixed valency: molecular wires and switches, *Chem. Soc. Rev.* 24 (1995) 121–134.
- [7] (a) K. Nakatani, J.A. Delaire, Reversible photoswitching of second-order nonlinear optical properties in an organic photochromic crystal, *Chem. Mater.* 9 (1997) 2682–2684; (b) S.L. Gilat, S.H. Kawai, J.-M. Lehn, Light-triggered molecular devices: photochemical switching of optical and electrochemical properties in molecular wire type diarylethene species, *Chem. Eur. J.* 1 (1995) 275–284; (c) A. Fernandez-Acebes, J.-M. Lehn, Optical switching and fluorescence modulation properties of photochromic metal complexes derived from dithienylethene ligands, *Chem. Eur. J.* 5 (1999) 3285–3292.
- [8] (a) B.J. Coe, S. Houbrechts, I. Asselberghs, A. Persoons, Efficient, reversible redox-switching of molecular first hyperpolarizabilities in ruthenium(II) complexes possessing large quadratic optical nonlinearities, *Angew. Chem., Int. Ed.* 38 (1999) 366–369; (b) B.J. Coe, J.A. Harris, L.A. Jones, B.S. Brunschwig, K. Song, K. Clays, J. Garin, J. Orduña, S.J. Coles, M.B. Hursthouse, Syntheses and properties of two-dimensional charged nonlinear optical chromophores incorporating redox-switchable cis-tetraammineruthenium(II) centers, *J. Am. Chem. Soc.* 127 (2005) 4845–4859.
- [9] (a) C.L. Hill, C.M. Prosser-McCartha, Homogeneous catalysis by transition metal oxygen anion clusters, *Coord. Chem. Rev.* 143 (1995) 407–455; (b) R. Neumann, Polyoxometalate complexes in organic oxidation chemistry, *Prog. Inorg. Chem.* 47 (1998) 317–370; (c) R. Neumann, A.M. Khenkin, Molecular oxygen and oxidation catalysis by phosphovanadomolybdates, *Chem. Commun.* (2006) 2529–2538.
- [10] (a) X. López, C. Bo, J.M. Poblet, Electronic properties of polyoxometalates: electron and proton affinity of mixed-addenda keggins and wells-dawson anions, *J. Am. Chem. Soc.* 124 (2002) 12574–12582; (b) H. Duclausaud, S.A. Borshch, Electron delocalization and magnetic state of doubly-reduced polyoxometalates, *J. Am. Chem. Soc.* 123 (2001) 2825–2829; (c) L.K. Yan, Z. Dou, W. Guan, S.Q. Shi, Z.M. Su, A DFT study on the electronic and redox properties of [PW<sub>11</sub>O<sub>39</sub>(ReN)]<sup>n−</sup> (n = 3, 4, 5) and [PW<sub>11</sub>O<sub>39</sub>(OsN)]<sup>2−</sup>, *Eur. J. Inorg. Chem.* (2006) 5126–5129.
- [11] W. Guan, G.C. Yang, C.G. Liu, P. Song, L. Fang, L.K. Yan, Z.M. Su, Reversible redox-switching second-order optical nonlinearity in polyoxometalate: a quantum chemical study of [PW<sub>11</sub>O<sub>39</sub>(ReN)]<sup>n−</sup> (n = 3–7), *Inorg. Chem.* 47 (2008) 5245–5252.
- [12] G. te Velde, F.M. Bickelhaupt, S.J.A. van Gisbergen, C. Fonseca Guerra, E.J. Baerends, J.G. Snijders, T. Ziegler, Chemistry with ADF, *J. Comput. Chem.* 22 (2001) 931–967.
- [13] C. Fonseca Guerra, J.G. Snijders, G. te Velde, E.J. Baerends, Towards an order-N DFT method, *Theor. Chem. Acc.* 99 (1998) 391–403.
- [14] ADF2008.01, SCM, Theoretical Chemistry, Vrije Universiteit, Amsterdam, The Netherlands, (2008), <http://www.scm.com>.
- [15] E. van Lenthe, E.J. Baerends, J.G. Snijders, Relativistic regular two-component Hamiltonians, *J. Chem. Phys.* 99 (1993) 4597–4610.
- [16] E. van Lenthe, A.E. Ehlers, E.J. Baerends, Geometry optimizations in the zero order regular approximation for relativistic effects, *J. Chem. Phys.* 110 (1999) 8943–8953.
- [17] S.H. Vosko, L. Wilk, M. Nusair, Accurate spin-dependent electron liquid correlation energies for local spin density calculations: a critical analysis, *Can. J. Phys.* 58 (1980) 1200–1211.
- [18] A.D. Becke, Density-functional exchange-energy approximation with correct asymptotic behavior, *Phys. Rev. A* 38 (1988) 3098–3100.
- [19] J.P. Perdew, Density-functional approximation for the correlation energy of the inhomogeneous electron gas, *Phys. Rev. B* 33 (1986) 8822–8824, Erratum: *Phys. Rev. B* 34 (1986) 7406–7406.
- [20] C.C. Pye, T. Ziegler, E. van Lenthe, J.N. Louwen, An implementation of the conductor-like screening model of solvation within the Amsterdam density

- functional package. Part II. COSMO for real solvents, *Can. J. Chem.* 87 (2009) 790–797.
- [21] S.Z. Hu, Z.H. Zhou, K.R. Tsai, Average van der Waals radii of atoms in crystals, *Acta Phys. -Chim. Sin.* 19 (2003) 1073–1077.
- [22] R. van Leeuwen, E.J. Baerends, Exchange-correlation potential with correct asymptotic-behavior, *Phys. Rev. A* 49 (1994) 2421–2431.
- [23] P.R.T. Schipper, O.V.S. Gritsenko, J.A. van Gisbergen, E.J. Baerends, Molecular calculations of excitation energies and hyperpolarizabilities with a statistical average of orbital model exchange-correlation potentials, *J. Chem. Phys.* 112 (2000) 1344–1352.
- [24] M. Grüning, O.V. Gritsenko, S.J.A. Gisbergen, E.J. Baerends, Shape corrections to exchange-correlation potentials by gradient-regulated seamless connection of model potentials for inner and outer region, *J. Chem. Phys.* 114 (2001) 652–660.
- [25] G.C. Yang, W. Guan, L.K. Yan, Z.M. Su, L. Xu, E.B. Wang, Theoretical study on the electronic spectrum and the origin of remarkably large third-order nonlinear optical properties of organoimide derivatives of hexamolybdates, *J. Phys. Chem. B* 110 (2006) 23092–23098.
- [26] M.J. Frisch, G.W. Trucks, H.B. Schlegel, Gaussian 03, Revision C.02, Gaussian Inc., Wallingford, CT, 2004.
- [27] X. López, J.A. Fernández, J.M. Poblet, Redox properties of polyoxometalates: new insights on the anion charge effect, *Dalton Trans.* (2006) 1162–1167.
- [28] J.A. Fernández, X. López, C. Bo, C. de Graaf, E.J. Baerends, J.M. Poblet, Polyoxometalates with internal cavities: redox activity, basicity, and cation encapsulation in  $[X^{n+}P_5W_{30}O_{110}]^{(15-n)-}$  preyssler complexes, with  $X = Na^+, Ca^{2+}, Y^{3+}, La^{3+}, Ce^{3+}$ , and  $Th^{4+}$ , *J. Am. Chem. Soc.* 129 (2007) 12244–12253.
- [29] S. Romo, J.A. Fernández, J.M. Maestre, B. Keita, L. Nadjo, C. de Graaf, J.M. Poblet, Density functional theory and ab initio study of electronic and electrochemistry properties of the tetranuclear sandwich complex  $[Fe^{III}_4(H_2O)_2(PW_9O_{34})_2]^{6-}$ , *Inorg. Chem.* 46 (2007) 4022–4027.
- [30] C.P. Kelly, C.J. Cramer, D.G. Truhlar, Aqueous solvation free energies of ions and ion–water clusters based on an accurate value for the absolute aqueous solvation free energy of the proton, *J. Phys. Chem. B* 110 (2006) 16066–16081.
- [31] F. Meyers, S.R. Marder, B.M. Pierce, J.L. Brédas, Electric field modulated nonlinear optical properties of donor–acceptor polyenes: sum-over-states investigation of the relationship between molecular polarizabilities ( $\alpha$ ,  $\beta$ , and  $\gamma$ ) and bond length alternation, *J. Am. Chem. Soc.* 116 (1994) 10703–10714.
- [32] L.G.S. Brooker, R.H. Sprague, Color and constitution. IV.1 The Absorption of phenol blue, *J. Am. Chem. Soc.* 63 (1941) 3214–3215.
- [33] L.G.S. Brooker, A.C. Craig, D.W. Heseltine, P.W. Jenkins, L.L. Lincoln, Color and constitution. XIII.1 Merocyanines as solvent property indicators, *J. Am. Chem. Soc.* 87 (1965) 2443–2450.
- [34] F.L. Huyskens, P.L. Huyskens, A.P. Persoons, Solvent dependence of the first hyperpolarizability of p-nitroanilines: differences between nonspecific dipole–dipole interactions and solute–solvent H-bonds, *J. Chem. Phys.* 108 (1998) 8161–8171.
- [35] S. Di Bella, I. Fragalà, Two-dimensional characteristics of the second-order nonlinear optical response in dipolar donor–acceptor coordination complexes, *New J. Chem.* 26 (2002) 285–290.
- [36] S. Di Bella, I. Fragalà, I. Ledoux, J. Zyss, Dipolar donor–acceptor-substituted schiff base complexes with large off-diagonal second-order nonlinear optical tensor components, *Chem. Eur. J.* 7 (2001) 3738–3743.